



# Divergent drivers of the spatial variation in greenhouse gas concentrations and fluxes along the Rhine River and the Mittelland Canal in Germany

Ricky Mwangada Mwanake<sup>1</sup> · Hannes Klaus Imhof<sup>1</sup> · Ralf Kiese<sup>1</sup>

Received: 18 December 2023 / Accepted: 16 April 2024  
© The Author(s) 2024

## Abstract

Lotic ecosystems are sources of greenhouse gases (GHGs) to the atmosphere, but their emissions are uncertain due to longitudinal GHG heterogeneities associated with point source pollution from anthropogenic activities. In this study, we quantified summer concentrations and fluxes of carbon dioxide (CO<sub>2</sub>), methane (CH<sub>4</sub>), nitrous oxide (N<sub>2</sub>O), and dinitrogen (N<sub>2</sub>), as well as several water quality parameters along the Rhine River and the Mittelland Canal, two critical inland waterways in Germany. Our main objectives were to compare GHG concentrations and fluxes along the two ecosystems and to determine the main driving factors responsible for their longitudinal GHG heterogeneities. The results indicated that the two ecosystems were sources of GHG fluxes to the atmosphere, with the Mittelland Canal being a hotspot for CH<sub>4</sub> and N<sub>2</sub>O fluxes. We also found significant longitudinal GHG flux discontinuities along the mainstems of both ecosystems, which were mainly driven by divergent drivers. Along the Mittelland Canal, peak CO<sub>2</sub> and CH<sub>4</sub> fluxes coincided with point pollution sources such as a joining river tributary or the presence of harbors, while harbors and in-situ biogeochemical processes such as methanogenesis and respiration mainly explained CH<sub>4</sub> and CO<sub>2</sub> hotspots along the Rhine River. In contrast to CO<sub>2</sub> and CH<sub>4</sub> fluxes, N<sub>2</sub>O longitudinal trends along the two lotic ecosystems were better predicted by in-situ parameters such as chlorophyll-*a* concentrations and N<sub>2</sub> fluxes. Based on a positive relationship with N<sub>2</sub> fluxes, we hypothesized that in-situ denitrification was driving N<sub>2</sub>O hotspots in the Canal, while a negative relationship with N<sub>2</sub> in the Rhine River suggested that coupled biological N<sub>2</sub> fixation and nitrification accounted for N<sub>2</sub>O hotspots. These findings stress the need to include N<sub>2</sub> flux estimates in GHG studies, as it can potentially improve our understanding of whether nitrogen is fixed through N<sub>2</sub> fixation or lost through denitrification.

**Keywords** N<sub>2</sub> fluxes · Harbors · External inputs · Metabolism rates · N fixation · Denitrification

---

Responsible Editor: Gerhard Lammel

✉ Ricky Mwangada Mwanake  
ricky.mwanake2@kit.edu

Hannes Klaus Imhof  
hannes.imhof@kit.edu

Ralf Kiese  
ralf.kiese@kit.edu

<sup>1</sup> Karlsruhe Institute of Technology, Institute for Meteorology and Climate Research, Atmospheric Environmental Research (IMK-IFU), Kreuzackbahnstrasse 19, 82467 Garmisch-Partenkirchen, Germany

## Introduction

Inland waters, comprising lotic (e.g., streams, rivers, and canals) and lentic (e.g., reservoirs, lakes, and ponds) ecosystems, are increasingly recognized as significant sources of greenhouse gases (GHGs), contributing ~15% (median: 8.3; interquartile range: 5.7–12.7 Pg CO<sub>2</sub>-eq based on a global warming potential of 100 years) to the total global carbon dioxide equivalent (CO<sub>2</sub>-eq) emissions (Jones et al. 2023; Lauerwald et al. 2023). In comparison, lotic ecosystems are characterized by disproportionately higher CO<sub>2</sub>-eq emissions (>60%) than lentic ecosystems, linked to their close connectivity to terrestrial landscapes and their turbulent flow conditions, which favors gas evasion to the atmosphere (Raymond et al. 2013; Rocher-Ros et al. 2023; Yao et al. 2020). The GHG concentrations and fluxes of lotic ecosystems are

also highly heterogeneous in space due to the variable nature of surrounding landscapes affecting local biogeochemical processes and differences in channel geomorphologies (e.g., Ho et al. 2022; Mwanake et al. 2022; Park et al. 2023; Teodoru et al. 2015), both of which may introduce significant uncertainties to GHG emission estimates from inland waters if not precisely quantified.

While research has demonstrated that headwaters, the inception points of river networks, contribute more than two-thirds of the global GHG emissions from riverine ecosystems (e.g., Li et al. 2021; Liu et al. 2022), anthropogenic activities along large rivers may modify this trend. Previous studies have shown that nutrients and carbon inputs from human-influenced landscapes to large rivers through diffuse and point sources favor in-situ GHG production processes such as nitrification, incomplete denitrification, methanogenesis, and respiration, creating GHG hotspots comparable to or higher than those from headwater streams (Borges et al. 2018; Mwanake et al. 2019; Park et al. 2018; Mwanake et al. 2023a, b). For instance, Mwanake et al. (2023a) reported higher or comparable GHG emissions from temperate rivers in Germany relative to small streams linked to inorganic nitrogen (N) and labile carbon (C) inputs from surrounding upstream cropland and urban areas. Similar findings were also found along the Seine River downstream of wastewater treatment plants (WWTPs) in large metropolitan areas in France (Marescaux et al. 2018). Apart from pollution sources related to surrounding landscapes and wastewater treatment plant effluents, the presence of harbors along large rivers, characterized by low-flow velocities, has also been shown to promote organic carbon accumulation and anoxic conditions, which favor methane (CH<sub>4</sub>) production hotspots through increased methanogenesis (Bussmann et al. 2022). Despite the importance of these local GHG hotspots along large rivers, field studies incorporating multiple measurements of GHG fluxes along river transects are still limited (but see Begum et al. 2021; Leng et al. 2023; Park et al. 2023), making it challenging to understand the critical drivers and magnitude of their longitudinal GHG flux heterogeneities.

Drainage ditches and canals, whose GHG dynamics are often understudied compared to rivers, have also been shown to be potent GHG hotspots of mainly CH<sub>4</sub> emissions due to their low-flow velocities that provide suitable anaerobic conditions for CH<sub>4</sub> production. It is estimated that these canals contribute ~3% of the global anthropogenic CH<sub>4</sub> emissions (Peacock et al. 2021), while they can also be hotspots of nitrous oxide (N<sub>2</sub>O) emissions, especially when they receive N inputs from surrounding landscapes (Reay et al. 2003). Like rivers, diffuse and point pollution sources along canal ecosystems may also result in significant longitudinal GHG heterogeneities. However, these pollution effects remain uncertain, as most studies often take single reach-scale

samples along canals to represent whole channel GHG magnitudes (Peacock et al. 2021).

Apart from GHG hotspots directly linked to allochthonous nutrients and carbon inputs, increased water-column primary production, especially during warm periods of the year, may also alter longitudinal GHG trends along large lotic ecosystems with relatively low water flow conditions. Although the influence of primary producers on lotic GHG concentrations remains uncertain due to the scarcity of studies with paired measurements of GHG concentrations and river metabolism rates (Battin et al. 2023), several potential mechanisms can be hypothesized linked to their effects on nutrient and carbon cycling. The decomposition of organic matter could supply fresh and more labile autochthonous organic carbon (C), favoring GHG production through C and N cycling processes. At the same time, N<sub>2</sub>-fixing cyanobacteria may contribute to excess mineral N, driving in-situ GHG production, particularly of N<sub>2</sub>O.

Conventional sampling approaches, which primarily focus on single locations along large rivers and canals, have been extensively applied to determine the magnitudes of their reach-scale GHG emissions (e.g., Mwanake et al. 2022; Peacock et al. 2021). Such approaches fail to capture the intricate nuances of large-scale longitudinal GHG dynamics along lotic ecosystems related to local GHG hotspots or coldspots (e.g., Silverthorn et al. 2023; Hotchkiss et al. 2015; Bussmann et al. 2022; Park et al. 2023; Teodoru et al. 2015), resulting in overestimation or underestimation of GHG fluxes from the entire ecosystems when the single measurements are upscaled over long distances. The lack of better spatial coverage in these large lotic ecosystems has been mainly driven by extensive resource requirements in making detailed longitudinal measurements along elongated reaches that can be hundreds of kilometers long. One approach that can overcome resource barriers is using high-precision and cost-effective sensors that simultaneously measure water quality parameters such as dissolved oxygen (DO), nutrients, and organic matter (OM) content (Bieroza et al. 2023). Combined with GHG concentration analysis, these sensors may constrict the critical drivers of longitudinal GHG flux discontinuities along lotic ecosystems, enhancing our capacity to model and manage these spatial GHG hotspots.

This study tested a novel sampling approach to quantify large-scale longitudinal GHG heterogeneities along one of the largest European rivers (Rhine River) and canal systems (Mittelland Canal) located in Germany. Within the framework of a river expedition, we explored a combined river and canal length of 632 km. Our approach encompassed longitudinal measurements of grab GHG samples (N<sub>2</sub>O, CO<sub>2</sub>, and CH<sub>4</sub>) and onsite sensor measurements of multiple water-physicochemical variables during the temperate summer. In addition, we also took grab samples

for  $N_2$  concentration analysis along both lotic ecosystems, which is a proxy for major N pathways (denitrification or biological  $N_2$  fixation) but currently remains understudied in large lotic ecosystems.

Our main objectives were (1) to compare GHG concentrations and fluxes from the Rhine River with the Mittelland Canal system; (2) to quantify large-scale longitudinal GHG heterogeneities along the two lotic ecosystems and infer the key drivers of these longitudinal GHG trends. We hypothesized that the canal would be characterized by much higher  $CH_4$  and  $N_2O$  fluxes than the river, driven by more anoxic conditions, point source inputs of nutrients, and availability of labile carbon from autotrophic processes. We also hypothesized that changes in either morphological, e.g., the existence of harbors with longer water residence times that favor internal C and N cycling or biogeochemical environmental conditions, would explain most of the longitudinal variabilities along both lotic ecosystems' mainstems.

## Materials and methods

### Study area

The Rhine River is among the ten largest rivers in Europe, with a total length of 1233 km and a catchment size of 185,500 km<sup>2</sup>. The river has its sources in the Swiss Alps, enters Lake Constance on the eastern part, crosses Lake Constance via Konstanz, and leaves it on the southwestern side. From Basel onward, the Rhine River flows towards the North Sea, and from here on, the Rhine is intensively used as an inland waterway and for hydropower production, traversing multiple landscapes with several major tributaries such as the Neckar, the Main, and the Mosel joining. This study was conducted on the German side of the Rhine River catchment, one of Germany's most important inland waterways, with a yearly transport volume of 6 million tons (Fig. 1). The first sampling point along the

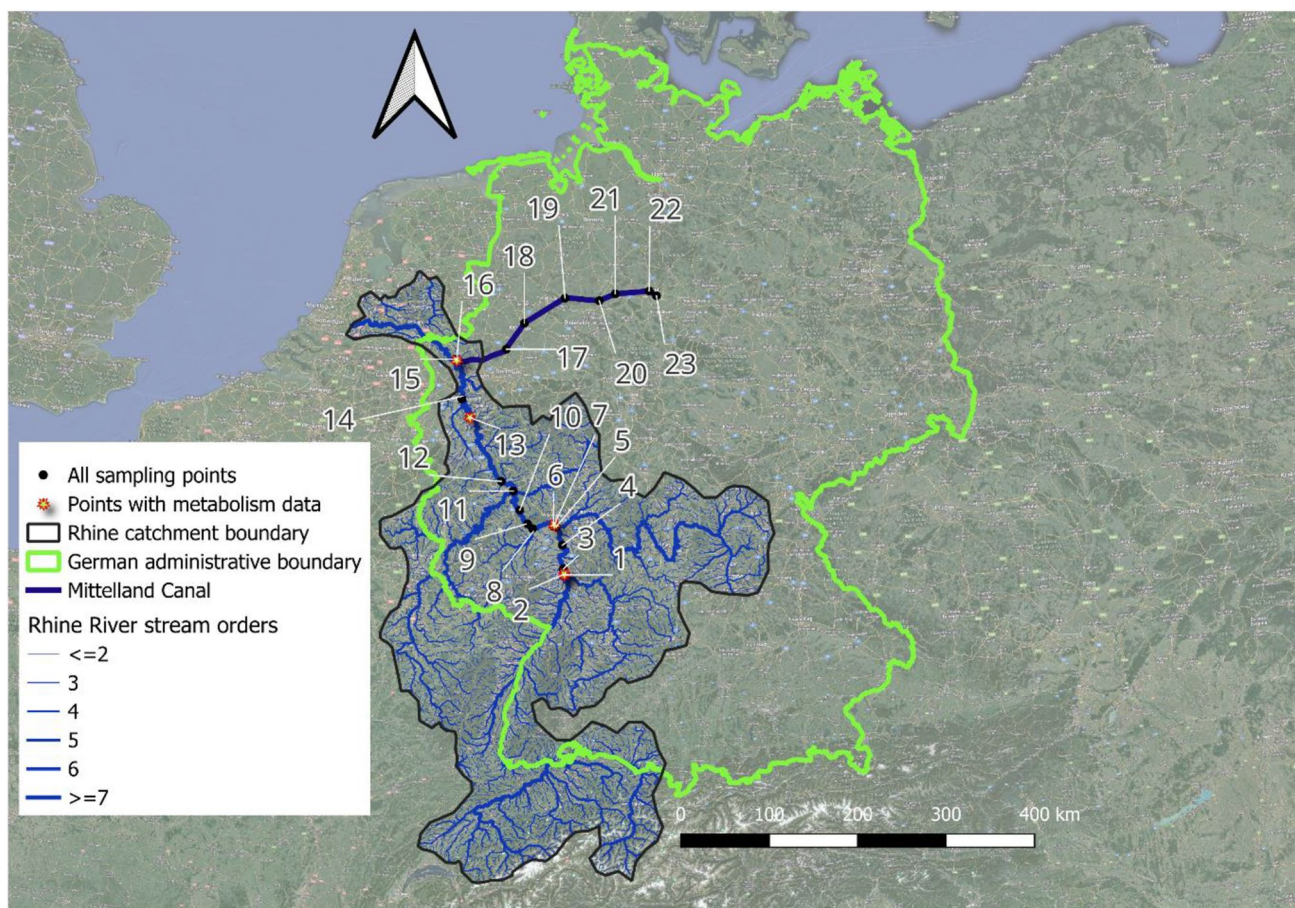


**Fig. 1** Map of the Rhine River network and the Mittelland Canal. The black dots and labels represent the 23 sampled sites with their site numbers (Table S1). The red star-shaped dots symbolize the water quality monitoring stations whose continuous oxygen and water tem-

perature datasets were used to calculate the metabolism rates of the Rhine River. The blue lines represent the Rhine River network, with the thickness and color intensity of the lines indicating stream size/order increases. The background map is from Google Earth

Rhine River was located at the midsection of the river (Mannheim, 653 km from the source), while our most downstream location was at Wesel, Germany (1023 km from the source; Table S1; Fig. 1).

The Mittelland Canal traverses Germany from west to east. It is one of the central connections of the industrialized areas in the northern Ruhr area to the large harbors of the North Sea (e.g., Rotterdam, Antwerpen, Amsterdam). In addition to the Rhine and Neckar, the Mittelland Canal is one of Germany's most important inland waterways and has a yearly transport volume of 6 million tons. Six large locks are located between sites 16 and 23 in Friedrichsfeld, Hünxe, Dorsten, Flaesheim, Ahsen, and Datteln (Fig. 1). These locks control the water flow within the canal by pumping water in and out, assisting the movement of large ships from west to east. Apart from its use as an inland waterway, the Mittelland Canal is part of the water distribution network in Germany. Specifically, freshwater is transported from the Lippe, the lower Ruhr, and the Rhine Rivers to the east, where it is used for industries and irrigation. According to a report by a local environmental agency, the Mittelland Canal is considered highly eutrophic due to point-source inputs of nutrients from several WWTPs and rivers, such as the Weser, along its longitudinal cross section (Landesumweltamt Nordrhein-Westfalen 2002).

### Sampling strategy

In this study, sampling was performed from 12.06.2023 to 06.07.2023, mostly between 9:00 am and 5:00 pm, on the Science and Media Vessel ALDEBARAN run by the German Ocean Foundation (Table S1; Figure S1). The field campaign was part of a more extensive field expedition, which aimed at connecting actors from society, business, and politics concerning the traces of human influences on water quality and biodiversity along the Rhine. A total of 23 lotic sites were sampled, comprising 16 sites (including four harbors) along the Rhine River (386-km stretch) that represented large (> 7) stream sizes/orders and seven canal sites (including two harbors) along the Mittelland Canal (246-km stretch, Table S1; Fig. 1).

### Analysis of water and gas samples

River and canal water was collected with a bucket from a depth of ~1 m below the water surface and sampled for ammonium, GHGs (CO<sub>2</sub>, N<sub>2</sub>O, and CH<sub>4</sub>), and N<sub>2</sub> concentrations. Samples for ammonium measurements were taken from the bucket and temporarily stored in a falcon tube. Analysis of ammonium (NH<sub>4</sub>-N) was done immediately in the field using a pHPhotoFlex Turb (WTW Germany) and the ammonium cuvette test A6/25 (173700, WTW Germany). For GHGs, triplicate samples were drawn from one bucket of water using the headspace

equilibration technique (Aho and Raymond 2019). In brief, 80 mL of water was equilibrated with 20 mL of atmospheric air in a syringe after shaking for 2 min in the bucket to maintain in-situ temperatures. The headspace gas samples were transferred into pre-evacuated 10-mL glass vials for GHG concentration analysis in the laboratory using an SRI gas chromatograph (8610C, Germany) with an electron capture detector (ECD) for N<sub>2</sub>O and a flame ionization detector (FID) with an upstream methanizer for simultaneous measurements of CH<sub>4</sub> and CO<sub>2</sub> concentrations. Dissolved GHG concentrations in the river and canal water were calculated from post-equilibration gas concentrations in the headspace after correcting for atmospheric (ambient) GHG concentrations (see Mwanake et al. 2022).

Duplicate water samples for N<sub>2</sub> concentration measurements were collected from the bucket in gas-tight 12-mL exetainers (Labco, UK) without air bubbles and stored in a refrigerator until analysis. In the laboratory, measurements of dissolved N<sub>2</sub> were carried out on a membrane inlet mass spectrophotometer (MIMS; Bay instruments, USA) at close to in-situ temperatures (~20 °C) following the procedure outlined in Kana et al. (1994). In brief, the MIMS measurements involved continuous uptake of the water samples through a gas-permeable silicone membrane using a peristaltic pump and detecting N<sub>2</sub> (mass 28) on a quadrupole mass spectrophotometer (Pfeiffer vacuum PrismaPlus). We used N<sub>2</sub>:Ar current ratios to measure N<sub>2</sub> concentrations with high precision (<0.05 CV%) (Kana et al. 1994; An et al. 2001). The MIMS setup included a liquid N<sub>2</sub> trap and a reduction furnace to minimize water vapor interference and other dissolved gases on the N<sub>2</sub> measurements (Kana et al. 1994).

### GHG and N<sub>2</sub> flux estimation

The daily diffusive GHG and N<sub>2</sub> fluxes ( $F$ ) (moles m<sup>-2</sup> d<sup>-1</sup>) for each of the sampling points were estimated using Fick's Law of gas diffusion (Eq. 1), where  $F$  is the product of the gas transfer velocity ( $k$ ) (m d<sup>-1</sup>) and the difference between the stream water concentrations ( $C_{sw}$ ) (moles m<sup>-3</sup>) and the ambient atmospheric gas concentration in water assuming equilibrium with the atmosphere ( $C_{sat}$ ) (moles m<sup>-3</sup>).

$$F = k(C_{sw} - C_{sat}) \quad (1)$$

The temperature-specific gas transfer velocities ( $k$ ) of CO<sub>2</sub>, CH<sub>4</sub>, N<sub>2</sub>O, and N<sub>2</sub> in Eq. 1 were calculated from normalized gas transfer velocities ( $k_{600}$ ) (m d<sup>-1</sup>) of each site- and temperature-dependent Schmidt numbers ( $Sc$ ) (unitless) of the respective gases (Eq. 2) (Raymond et al. 2012).

$$k = k_{600} \times \left( \frac{600}{Sc} \right)^{0.5} \quad (2)$$

The  $k_{600}$  values of each of the sampling points were predicted using Eq. 3 adapted from Raymond and Cole (2001),

where  $U_{10}$  is the windspeed at 10 m ( $\text{m s}^{-1}$ ) above the water surface and 0.24 is a unit conversion factor, i.e., from  $\text{cm h}^{-1}$  gas transfer velocities to  $\text{m d}^{-1}$ .

$$k_{600} = 1.91e^{0.35U_{10}} \times 0.24 \quad (3)$$

Site-specific windspeeds in this study were drawn from the E-OBS gridded morphological data for Europe, representing daily averages of the exact dates for each sampling point (Cornes et al. 2018; <https://cds.climate.copernicus.eu/cdsapp#!/dataset/insitu-gridded-observations-europe?tab=overview>, accessed on 28.02.2024). The final fluxes were then expressed in mass units by multiplying by the respective molar masses.

### Sensor measurements of water-physicochemical properties

Onsite measurements of water-physicochemical properties such as  $\text{NO}_3\text{-N}$ , total organic carbon (TOC), total suspended solids (TSS), dissolved organic carbon (DOC), chlorophyll-*a*, UV254, and UV254f were performed simultaneously with the grab samples using a calibrated optical sensor (S::Can spectro::lyser V3, Messtechnik GmbH, Vienna, Austria). The specific ultraviolet absorbance at 254 nm ( $\text{SUVA}_{254}$ , a measure of DOC quality) was calculated by dividing UV254 by DOC concentrations to estimate DOC aromaticity (e.g., Bodmer et al. 2016). Additional water parameters such as pH, conductivity, water temperature, atmospheric pressure, and dissolved oxygen were also monitored using a locally calibrated multiprobe (YSI ProDSS probe, USA). The S::Can and the YSI ProDSS probes were mounted at the back of the ship in a bucket with a volume of  $\sim 20$  L and an overflow pipe. Water inflow was maintained by a freshwater pump from  $\sim 1$ -m depth with a water flow rate of  $\sim 12.7$  L/min (Figure S1).

### Estimation of $k_{600}$ , ecosystem respiration, and gross primary production rates along the Rhine River

We used continuous hourly data (12.06.23–30.06.23) of dissolved oxygen (DO) and water temperature from four water quality monitoring stations along the Rhine River for the estimation of normalized gas transfer velocities ( $k_{600}$ :  $\text{m d}^{-1}$ ), ecosystem respiration (ER), and gross primary production (GPP) rates in  $\text{g O}_2 \text{ m}^{-2} \text{ d}^{-1}$ . The dataset was sourced from continuous water quality monitoring stations of the NRW State Agency for Nature, Environment and Consumer Protection (LANUV) for the Wasserkontrollstation Rhine-North Kleve-Bimmen (00504) and Rhine South Bad Honnef (00103) and from the State Office for the Environment Rhineland-Palatinate (LFU RLP) for the “Rheingütestation Worms” ([\[on.de\]\(https://www.rheinguetestati.on.de\)\) and the “Rheinwasser Untersuchungsstation Mainz-Wiesbaden” \(<https://www.rheinwasseruntersuchungsstation.de/>\). The modeling of these parameters from the hourly DO measurements was done using a Bayesian model built in the “StreamMetabolizer” R package \(Appling et al. 2018\). Final daily estimates of  \$k\_{600}\$ , GPP, and ER rates for the four sites were calculated by averaging daily estimates of the duration of our sampling campaign \(22-day average\). In addition, we also calculated net ecosystem production \(NEP\) rates as the difference between GPP and ER.](https://www.rheinguetestati</a></p>
</div>
<div data-bbox=)

### Statistical analysis

Analysis of variance from significant ( $p$ -value  $< 0.05$ ) linear regression models followed by a Tukey post hoc analysis of least square means were performed to determine the combined importance of lotic ecosystem type (river and canal) and the presence of harbors on the spatial variability of water-physicochemical variables, GHG and  $\text{N}_2$  concentrations, and fluxes (“R stats,” “emmeans,” and “multcomp” packages in R version 4.3.2). The performances of these linear models were assessed based on the distribution of their residuals; that is, they should be normally distributed with a mean close to zero, as well as the  $r^2$  of the regressions.

Apart from broader-scale drivers of spatial variation related to ecosystem type and harbors, longitudinal trends of the water-physicochemical variables, GHG and  $\text{N}_2$  concentrations, and fluxes in the two lotic ecosystems were also investigated by assessing their correlative relationships with downstream distance (Pearson correlation analysis using “ggplot2” and “ggpubr” packages in R version 4.3.2). To determine the biogeochemical drivers of the longitudinal trends in GHG fluxes, several bivariate linear regression analyses were performed, and a  $p$ -value threshold of  $< 0.05$  was applied to determine significant relationships (R stats package in R version 4.3.2). Bivariate relationships with  $p$ -values ranging from 0.05 to 0.10, which may have been insignificant due to our small sample sizes and high spatial variability in the dataset, were also considered to represent possible positive or negative trends with the GHG fluxes.

The dependent variables in the regression models were  $\text{CO}_2$ ,  $\text{CH}_4$ , and  $\text{N}_2\text{O}$  fluxes. The independent variables in the models were water temperature,  $\text{SUVA}_{254}$ , chlorophyll-*a*, DOC, TOC, TSS,  $\text{NH}_4\text{-N}$ ,  $\text{NO}_3\text{-N}$ , and  $\text{N}_2$  fluxes, which serve as direct or indirect indicators of GHG production or consumption processes. Additional independent variables such as GPP, ER, and NEP rates were used at four sites along the Rhine River where the data was available (see the “Materials and methods” section for details). Because all three GHG fluxes were not normally distributed, we transformed them using the natural logarithm to meet the normality assumption required for the regression models and also to improve model performance.

## Results

### Comparisons between the river and canal ecosystems

#### Water-physicochemical properties

Summertime water-physicochemical variables along the longitudinal transects of the two lotic ecosystems varied up to an order of magnitude, with SUVA<sub>254</sub> (a measure of DOC quality), chlorophyll-*a*, TOC, and TSS concentrations showing the highest variabilities, ranging from 4.34 to 35.35 L mg<sup>-1</sup>, 92.87 to 267.30 μg L<sup>-1</sup>, 3.56 to 55.05 mg L<sup>-1</sup>, and 4.64 to 273.74 mg L<sup>-1</sup>, respectively (Fig. 2). In contrast, water temperature and DOC concentrations had a narrower range of 19.26–28.20 °C and 1.94–5.09 mg L<sup>-1</sup>, respectively. Chlorophyll-*a*, DOC, SUVA<sub>254</sub>, TOC, and TSS were significantly higher in the Mittelland Canal than in the Rhine River (Table 1; Fig. 2).

Nitrate concentrations were generally an order of magnitude higher than NH<sub>4</sub>-N concentrations irrespective of ecosystem type, ranging from 3.91 to 13.27 mg L<sup>-1</sup> compared to 0.15–0.50 mg L<sup>-1</sup> for NH<sub>4</sub>-N (Fig. 2). Comparing the two lotic ecosystems, NO<sub>3</sub>-N concentrations were 1.4 times higher in the Mittelland Canal than in the Rhine River (Table 1; Table S2; Fig. 2). In contrast to NO<sub>3</sub>-N, NH<sub>4</sub>-N concentrations were not significantly different between the canal and the river system (Table 1; Fig. 2). The presence of harbors within both ecosystem types had no significant effects on all water quality parameters except for NO<sub>3</sub>-N concentrations in the Mittelland Canal, which were 2 times lower in the harbors than in the canal mainstem (Table 1; Table S2; Fig. 2).

#### Normalized gas transfer velocity, GHG and N<sub>2</sub> concentrations and fluxes

The  $k_{600}$  values modeled from the windspeed data ranged from 0.86 to 2.21 m d<sup>-1</sup> across all 23 sites. At the four stations along the Rhine River where  $k_{600}$  was also modeled from O<sub>2</sub> data, the mean and range of these values were within the same order of magnitude as the windspeed estimates, though the O<sub>2</sub>-based estimates had a higher mean and were more variable than the windspeed-based estimates (O<sub>2</sub> estimates: mean; 1.88, range; 1.47–2.21 m d<sup>-1</sup>; windspeed estimates: mean; 1.34, range; 1.23–1.38 m d<sup>-1</sup>).

In terms of emissions, the Rhine River and the Mittelland Canal were both sources of GHGs to the atmosphere indicated by their positive flux values (Fig. 3). Their concentrations and fluxes were also highly variable across the two ecosystems inclusive or exclusive of harbors, ranging up to two orders of magnitude, i.e., from 0.05 to 3.27 μmol

L<sup>-1</sup> and 0.52 to 50.29 mg m<sup>-2</sup> d<sup>-1</sup> for CH<sub>4</sub>-C, from 11.66 to 82.61 μmol L<sup>-1</sup> and 10.90 to 1133.60 mg m<sup>-2</sup> d<sup>-1</sup> for CO<sub>2</sub>-C, and from 5.92 to 44.56 nmol L<sup>-1</sup> and 0.03 to 1.45 mg m<sup>-2</sup> d<sup>-1</sup> for N<sub>2</sub>O-N (Fig. 3).

Methane concentrations and fluxes were ~5 times higher in the Mittelland Canal than in the Rhine mainstem. However, harbors along the Rhine created CH<sub>4</sub> hotspots, with CH<sub>4</sub> fluxes comparable to those quantified at the Mittelland Canal (Table 1; Table S2; Fig. 3). Even though ecosystem type and the presence of harbors had no significant effect on CO<sub>2</sub> and N<sub>2</sub>O concentrations and fluxes (Table 1), the mean CO<sub>2</sub> values tended to be lower in the harbors than in the mainstems of the Mittelland Canal and Rhine River, while the mean N<sub>2</sub>O concentrations and fluxes were ~2 times higher in the Mittelland Canal than in the Rhine River (Table S2; Fig. 3).

In contrast to the GHGs, N<sub>2</sub> fluxes in the two lotic ecosystems indicated either sinks or sources of the gas to the atmosphere based on their positive and negative values (Table S2; Fig. 3). N<sub>2</sub> concentrations and fluxes ranged from 462.08 to 522.20 μmol L<sup>-1</sup> and –1747.31 to 673.91 mg m<sup>-2</sup> d<sup>-1</sup>, respectively (Fig. 3). While neither ecosystem type nor harbors significantly affected N<sub>2</sub> concentrations and fluxes (Table 1), the highest negative N<sub>2</sub> fluxes equal to biological N<sub>2</sub> fixation were predominantly found in the Rhine River (Fig. 3).

#### Estimated GPP, ER, and NEP rates from continuous hourly O<sub>2</sub> data

At the four sites along the mainstem of the Rhine River, the estimated daily mean GPP, ER, and NEP rates for the duration of our study ranged from 1.59 to 7.33, –6.57 to –5.02, and –4.31 to 0.75 g O<sub>2</sub> m<sup>-2</sup> d<sup>-1</sup>, respectively (Fig. 4). GPP, ER, and NEP rates increased downstream, with correlation coefficients ranging from 0.87 to 0.91 (Fig. 4A, B, C). These increasing trends were also found for water-physicochemical properties such as NH<sub>4</sub>-N, chlorophyll-*a*, and TOC concentrations, with significant correlation coefficients ranging from 0.68 to 0.73.

#### Longitudinal GHG trends along the two lotic ecosystems not linked to harbors

The presence of harbors resulted in discontinuities in the longitudinal GHG trends along the Rhine River, particularly for CO<sub>2</sub> and CH<sub>4</sub> concentrations and fluxes (Fig. 5). That said, the spatial heterogeneities of the GHG fluxes along the Rhine mainstem were still significant even when harbor sites were excluded, with coefficient of variation (CV) values of 39% for CO<sub>2</sub>, 79% for CH<sub>4</sub>, and 91% for N<sub>2</sub>O.

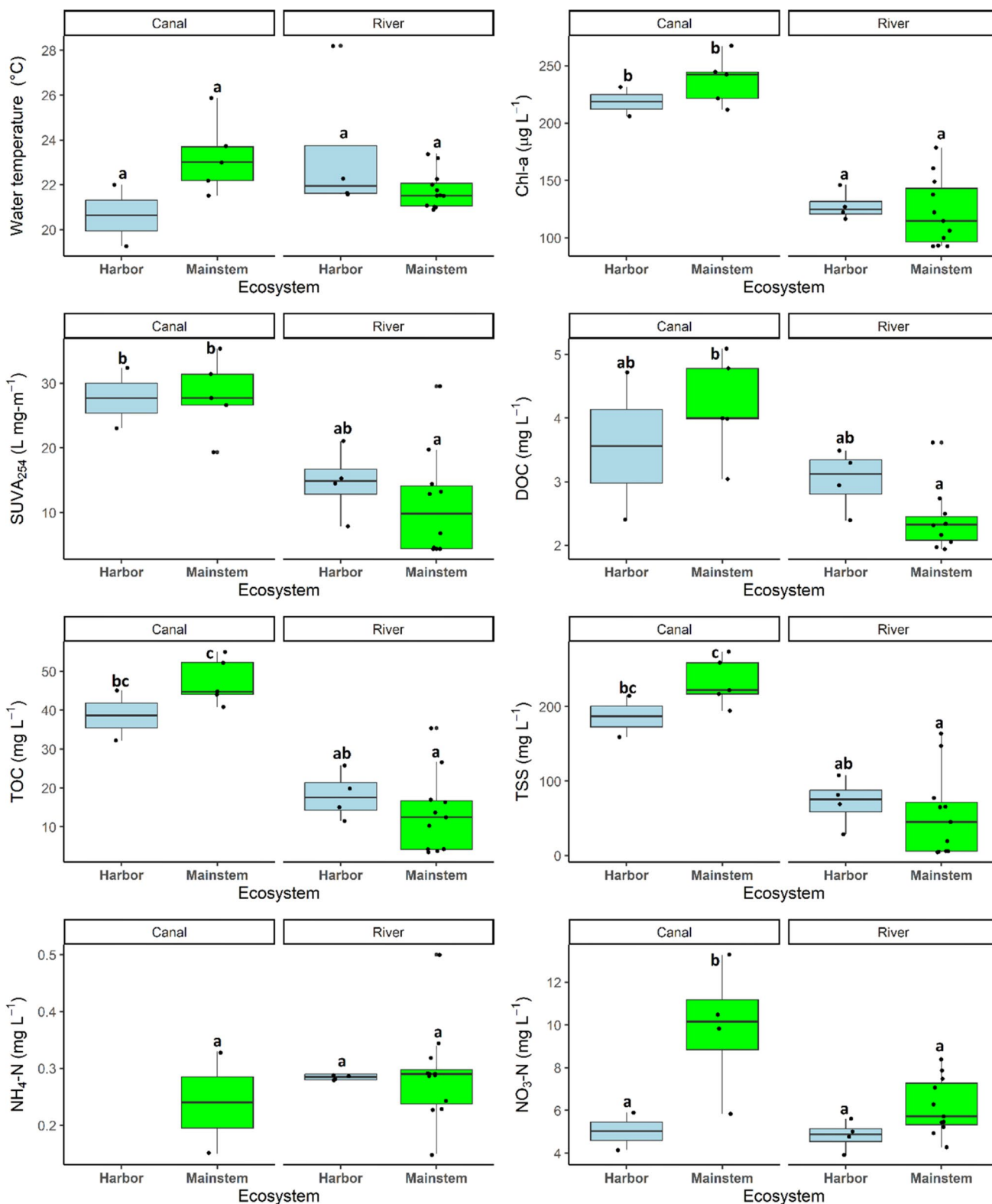


**Fig. 2** Boxplots indicating the interactive effect of lotic ecosystem type and harbor presence on the spatial variability of water-physico-chemical properties. Black dots represent the individual data points

for each site. The letters on top of the boxplots indicate the significant differences from Tukey post hoc analysis of least square means from the regression models (Table 1)

**Table 1** Analysis of variance results from linear regression models predicting the interactive effect of lotic ecosystem type (river vs. canal) and presence of harbors on water-physicochemical properties, GHG and N<sub>2</sub> concentrations, and fluxes

Independent variable	df	ANOVA from linear regression models		
		F-statistic	p-value	r <sup>2</sup>
Water temperature (°C)	3	2.21	0.121	
Chl- <i>a</i> (µg L <sup>-1</sup> )	3	19.20	<0.001	0.72
SUVA <sub>254</sub> (L mg <sup>-1</sup> m <sup>-1</sup> )	3	7.34	0.002	0.49
DOC (mg L <sup>-1</sup> )	3	7.82	0.002	0.51
TOC (mg L <sup>-1</sup> )	3	19.50	<0.001	0.73
TSS (mg L <sup>-1</sup> )	3	18.41	<0.001	0.71
NH <sub>4</sub> -N (mg L <sup>-1</sup> )	3	0.33	0.727	
NO <sub>3</sub> -N (mg L <sup>-1</sup> )	3	7.18	0.003	0.48
CO <sub>2</sub> (µmol L <sup>-1</sup> )	3	1.00	0.415	
CO <sub>2</sub> -C flux (mg m <sup>-2</sup> d <sup>-1</sup> )	3	0.82	0.501	
CH <sub>4</sub> (µmol L <sup>-1</sup> )	3	14.33	<0.001	0.65
CH <sub>4</sub> -C flux (mg m <sup>-2</sup> d <sup>-1</sup> )	3	12.80	<0.001	0.62
N <sub>2</sub> O (µmol L <sup>-1</sup> )	3	1.34	0.291	
N <sub>2</sub> O-N (flux (mg m <sup>-2</sup> d <sup>-1</sup> ))	3	0.63	0.603	
N <sub>2</sub> (µmol L <sup>-1</sup> )	3	0.10	0.959	
N <sub>2</sub> flux (mg m <sup>-2</sup> d <sup>-1</sup> )	3	0.19	0.903	

Only the r<sup>2</sup> values of significant models (*p*-value < 0.05) are shown

Similar to the metabolism estimates and some water-physicochemical parameters, GHG concentrations and fluxes along the mainstem of the Rhine also showed correlative patterns with the distance from the Rhine's source, albeit not always significant (Pearson correlation coefficient; *p*-value > 0.05) (Fig. 4; Fig. 5). Carbon dioxide concentrations and fluxes tended to increase downstream, with the highest value found after the confluence with the Main River, which also had elevated chlorophyll-*a* and TOC concentrations (Fig. 4E, F; Fig. 5A, B). In contrast to CO<sub>2</sub>, CH<sub>4</sub> concentrations and fluxes decreased downstream, with the highest value found after the confluence with the Neckar River (Fig. 5C, D).

River confluences and harbors had less influence on the downstream trends of N<sub>2</sub>O, and thus, these trends were more unidirectional, with concentrations and fluxes showing significant increases with distance from the Rhines source (Fig. 5E, F). The increases in N<sub>2</sub>O concentrations and fluxes also coincided with simultaneous increases in NH<sub>4</sub>-N concentrations (Fig. 4D) but were contrary to N<sub>2</sub> concentration and N<sub>2</sub> flux trends, which declined with the distance from the Rhines source (Fig. 5G, H).

Compared to the Rhine River, the variation in GHG fluxes along the Mittelland Canal's mainstem was up to 2 times higher, with CV values of 83% for CO<sub>2</sub>, 89% for CH<sub>4</sub>, and 88% for N<sub>2</sub>O (Figure S2). The highest CH<sub>4</sub> concentrations and fluxes were found at a harbor site with low CO<sub>2</sub>

concentrations and fluxes, while the highest CO<sub>2</sub>, N<sub>2</sub>O, and N<sub>2</sub> concentrations and fluxes were found after the confluence with the Weser River (Figure S2).

### Biogeochemical controls on the longitudinal GHG flux trends along the Rhine River and the Mittelland Canal mainstems

We used bivariate linear regressions to reveal the most relevant biogeochemical drivers of the longitudinal GHG flux trends along the Rhine River and the Mittelland Canal mainstems. The regressions were based on GHG flux relationships with in-situ water-physicochemical variables and N<sub>2</sub> fluxes, as well as GPP, ER, and NEP rates available for the Rhine River (Table 2). At the Rhine, CO<sub>2</sub> fluxes were significantly positively related to ER rates, while CH<sub>4</sub> fluxes showed decreasing trends with the increase in NO<sub>3</sub>-N concentrations (Table 2). In contrast to CO<sub>2</sub> and CH<sub>4</sub>, the increasing trend of N<sub>2</sub>O fluxes with distance from the source was significantly predicted by most of the water-physicochemical properties and process rates that showed similar unidirectional trends (Table 2; Fig. 4). N<sub>2</sub>O fluxes were positively related to TOC and TSS concentrations and GPP and NEP rates and negatively related to N<sub>2</sub> fluxes (Table 2). N<sub>2</sub>O fluxes also showed an increasing trend with NH<sub>4</sub>-N concentrations, even though the relationship was insignificant (*p*-value 0.06).

Contrary to the Rhine River, the longitudinal GHG variability in the Mittelland Canal mainstem was much less correlated with water-physicochemical parameters. CO<sub>2</sub> fluxes showed no significant relationship with water-physicochemical properties and N<sub>2</sub> fluxes, while both CH<sub>4</sub> and N<sub>2</sub>O fluxes only showed significant positive relationships or just trends with N<sub>2</sub> fluxes (Table 2).

## Discussion

This study provided a spatially explicit dataset covering GHG concentration measurements and estimated fluxes of GHGs and N<sub>2</sub>, accompanied by measurements of various water-physicochemical properties in the Rhine River and Mittelland Canal, thus enabling the determination of important drivers of their longitudinal GHG flux heterogeneities. We found that summertime GHG fluxes in these two lotic ecosystems were always positive, contributing to the growing evidence that lotic ecosystems are significant sources of GHGs to the atmosphere (Lauerwald et al. 2023; Peacock et al. 2021; Rocher-Ros et al. 2023).

In agreement with our hypothesis, the Mittelland Canal, which has been reported to receive several inflows from WWTPs and river tributaries (Landesumweltamt Nordrhein-Westfalen 2002), had higher N<sub>2</sub>O and CH<sub>4</sub> fluxes than the

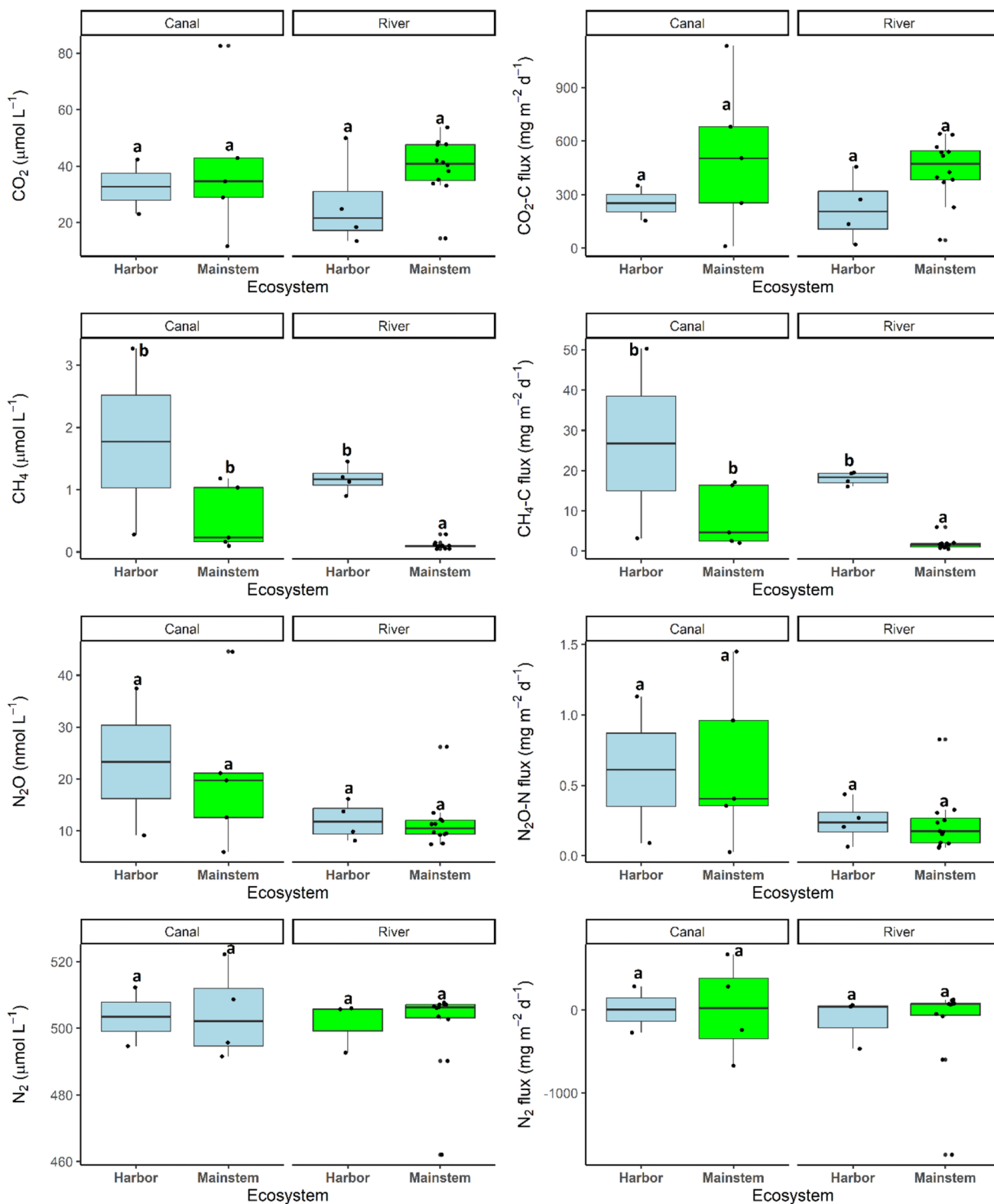


**Fig. 3** Boxplots indicating the interactive effect of lotic ecosystem type and the presence of harbors on the spatial variability of GHG and N<sub>2</sub> concentrations and fluxes. Black dots represent the individual

data points at each site. The letters on top of the boxplots indicate the significant differences from Tukey post hoc analysis of least square means from the regression models (Table 1)

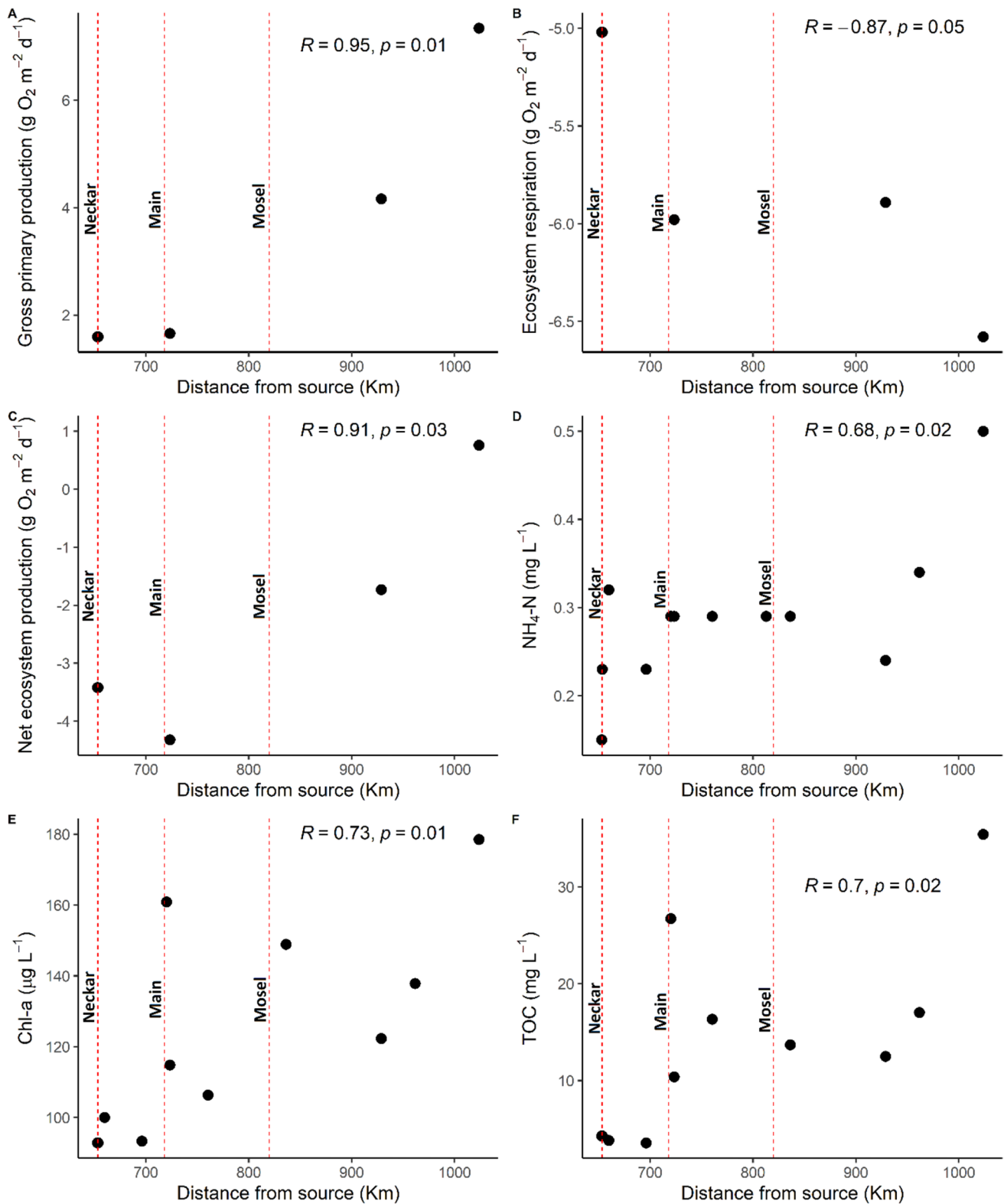


**Fig. 4** Longitudinal trends of **A, B,** and **C** GPP, ER, and NEP rates and **D, E,** and **F** NH<sub>4</sub>-N, chlorophyll-*a*, and TOC concentrations along the Rhine mainstem. The dotted lines on the graphs repre-

sent the inflow of major tributaries along the Rhine (Neckar, Main, Mosel). Text on the graphs shows the Pearson correlation coefficients ( $r$ ) and  $p$ -value of the longitudinal trends with downstream distance

Rhine River. We contend that these inflows likely contributed to elevated nutrients and labile organic carbon concentrations, which fueled in-situ  $N_2O$  and  $CH_4$  production processes or directly added externally sourced dissolved  $N_2O$  and  $CH_4$ , similar to what was found in other studies (Brown et al. 2023; Mwanake et al. 2023a; Zhang and Chadwick 2022).

The comparison of both lotic ecosystems showed that divergent drivers controlled longitudinal heterogeneities in the GHG fluxes. Spatial variability of GHG fluxes along the Rhine River was linked to harbors and site-specific biogeochemical process rates, agreeing with findings from previous studies (Hotchkiss et al. 2015; Busmann et al. 2022; Park et al. 2023; Mwanake et al. 2023a). For example, harbors at the Rhine River led to local hotspots of  $CH_4$  emission, which we linked to longer water residence times promoted by the still waters that favor organic matter and sediment accumulation, resulting in anoxic conditions and methane production. At the same time, the downstream increasing trends of  $N_2O$  and  $CO_2$  concentrations and fluxes were linked to either autotrophic or heterotrophic source processes inferred from in-situ estimates of  $N_2$  fluxes, as well as GPP, ER, and NEP rates.

In contrast to the Rhine River, most of the longitudinal GHG trends in the canal were challenging to predict from changes in in-situ water-physicochemical properties. This finding suggested that other factors not quantified in this study, such as point-pollution sources of GHGs, nutrients, and organic carbon, may have significantly controlled longitudinal GHG heterogeneities along the Mittelland Canal. Nevertheless, we did find that 90% of the  $N_2O$  flux spatial variability in the canal ecosystem was linked to  $N_2$  emissions. This result implied that denitrification was an essential source of  $N_2O$  in the canal, opposite to what we found in the Rhine River, where coupled  $N_2$  fixation and nitrification inferred from concurrent negative  $N_2$  fluxes and elevated  $NH_4-N$  concentrations may have accounted for  $N_2O$  flux hotspots. Overall, our findings suggested that single GHG measurements along large lotic ecosystems, which ignore local GHG hotspots linked to the presence of harbors, point pollution sources, or biogeochemical cycling, may result in significant uncertainties in entire ecosystem GHG emission estimates. This conclusion was particularly true for the canal ecosystem, which was characterized by higher and more spatially variable GHG concentrations and fluxes than the river ecosystem.

### Longitudinal discontinuities in $CO_2$ fluxes linked to harbors, point pollution sources, and metabolism rates

Carbon dioxide concentrations and fluxes quantified in this study are within the range of those quantified from other

studies in temperate ecosystems, as well as the global estimates (Lauerwald et al. 2015; Raymond et al. 2013), but are much lower than those quantified from heavily polluted Asian rivers (Begum et al. 2021). Previous studies in riverine ecosystems have found  $CO_2$  uptake during the temperate summer due to autotrophic  $CO_2$  fixation (Gómez-Gener et al. 2021). However, this study's daytime  $CO_2$  fluxes along the Rhine River were surprisingly positive throughout the summer campaign, suggesting that  $CO_2$  production via ER outweighed  $CO_2$  consumption via gross primary production (GPP). This conclusion is supported by the net ecosystem production (NEP) estimates from four sites along the Rhine that were primarily negative, indicating a net  $CO_2$  loss to the atmosphere.

Like the Rhine River, the Mittelland Canal also had positive  $CO_2$  fluxes, albeit slightly higher than the Rhine River. Judging by the higher carbon availability in the canal, one may assume that net in-situ heterotrophic processes were driving  $CO_2$  fluxes, similar to what we inferred for the Rhine. NEP estimates were unavailable for the Mittelland Canal, which did not allow us to link net heterotrophy to  $CO_2$  fluxes. However, based on a previous environmental report that indicated several inflows of treated wastewater or river tributaries into the Mittelland Canal (Landesumweltamt Nordrhein-Westfalen 2002), we hypothesized that the  $CO_2$  fluxes in the canal are likely driven by external dissolved  $CO_2$  supplies from these point-sources rather than internal production (e.g., Mwanake et al. 2023a). While it was difficult to indicate the contributions of WWTPs, we found that peak  $CO_2$  fluxes in the Mittelland Canal coincided with the inflow of the Weser River, agreeing with our hypothesis that external inflows of  $CO_2$  from a point pollution source likely contributed to the elevated  $CO_2$  fluxes in the canal.

Along the two large lotic ecosystems, longitudinal discontinuities in  $CO_2$  concentrations and fluxes were collectively linked to harbors, point pollution sources, and metabolism rates, similar to several other lotic studies (Begum et al. 2021; Deemer et al. 2016; Mwanake et al. 2023a). Within the Rhine River, harbor areas resulted in lower  $CO_2$  concentrations and fluxes than the river mainstem, which we attributed to their morphology that favors low-flow conditions, accumulation of organic matter, and anoxic conditions that limit aerobic respiration rates. This conclusion is further supported by the slightly higher DOC, TOC, and TSS concentrations in the harbors than in the mainstem of the Rhine.

Besides morphological controls, biogeochemical rates supported  $CO_2$  hotspots along the Rhine's mainstem. Previous fluvial studies have linked increased ER rates with organic carbon concentrations (Mulholland et al. 2001; Piatka et al. 2021; Stelzer et al. 2003). This study found a concurrent increase in downstream TOC and  $CO_2$  fluxes, suggesting that the increasing TOC favored instream  $CO_2$  production via favored ER rates. Furthermore, our study

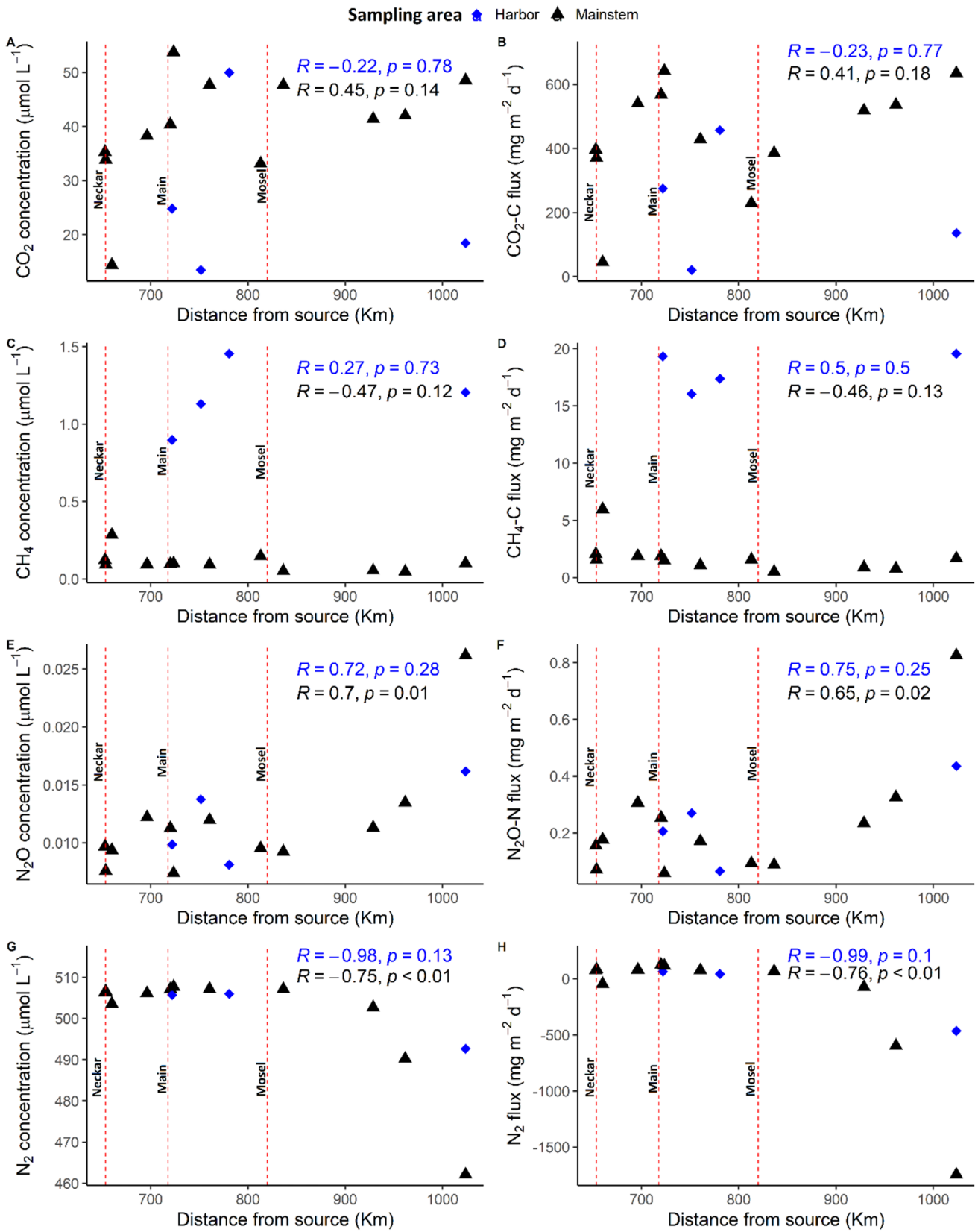


**Fig. 5** Longitudinal trends of CO<sub>2</sub>, CH<sub>4</sub>, N<sub>2</sub>O, and N<sub>2</sub> concentrations and fluxes along the Rhine River. Blue-colored points with diamond shapes indicate the harbor sites, while black-colored points with triangle shapes indicate the sites along the mainstem. The dotted lines on the graphs represent the inflow of major tributaries along the Rhine (Neckar, Main, Mosel). Text on the graphs shows the Pearson correlation coefficients (*r*) and *p*-value of the longitudinal trends with downstream distance

revealed a positive correlation between ER and CO<sub>2</sub> fluxes, which accounted for up to 88% of the downstream increasing trend that we found for the fluxes, strengthening this argument. In contrast to the Rhine River, the longitudinal trends in the Mittelland Canal were not predicted by any of our measured water-physicochemical properties, with peak CO<sub>2</sub> fluxes coinciding with the inflow of the Weser River.

### Longitudinal discontinuities in CH<sub>4</sub> fluxes linked to harbors and methanogenesis

Like CO<sub>2</sub>, riverine CH<sub>4</sub> concentrations and fluxes quantified here were mainly within the range of global estimates (Rocher-Ros et al. 2023). However, those quantified in the canal ecosystem were primarily at the higher end of the estimates. These findings strengthen the idea that canal ecosystems are hotspots for CH<sub>4</sub> emissions, similar to what has been found in previous studies (Peacock et al. 2021; Rocher-Ros et al. 2023).

The longitudinal variability of CH<sub>4</sub> concentrations and fluxes in the Rhine River was linked to both harbors and biogeochemical drivers. Contrary to CO<sub>2</sub>, harbor areas were hotspots for CH<sub>4</sub> fluxes, a finding agreeing with our earlier hypothesis that low-flow conditions and high organic matter accumulation in these areas likely favor anoxic conditions suitable for methanogenesis. A similar longitudinal study along the Elbe River also found higher CH<sub>4</sub> fluxes in harbor areas, alluding to similar controls of longer water residence time and high sediment and organic matter conditions favorable for methane production (Bussmann et al. 2022).

Methane variability was attributed to variable production rates via methanogenesis along the Rhine's mainstem. Several studies have shown that negative correlations between NO<sub>3</sub>-N and CH<sub>4</sub> imply methane production via methanogenesis, as NO<sub>3</sub>-N inhibits the processes as a terminal electron acceptor (TEA) (Baulch et al. 2011; Schade et al. 2016). Our study found a decreasing trend of CH<sub>4</sub> fluxes with NO<sub>3</sub>-N concentrations (*p*-value = 0.08), pointing out that methane production hotspots via methanogenesis along the Rhine may occur in areas with low TEA, such as NO<sub>3</sub>-N. Unlike CO<sub>2</sub>, CH<sub>4</sub> fluxes along the canal mainstem showed an increasing trend with N<sub>2</sub> fluxes (*p*-value = 0.10), suggesting that anoxic conditions that favor denitrification may also account for CH<sub>4</sub> production hotspots via methanogenesis.

### Longitudinal discontinuities in N<sub>2</sub>O fluxes linked to N transformation processes

Like CO<sub>2</sub> and CH<sub>4</sub>, riverine N<sub>2</sub>O fluxes fell within the global range of previous estimates from large rivers (Hu et al. 2016), with those from the Mittelland Canal comparable to N<sub>2</sub>O flux values from drainage ditches draining cropland landscapes laden by high NO<sub>3</sub> concentrations (Reay et al. 2003). The high NO<sub>3</sub> conditions in the Mittelland Canal relative to the Rhine River resulted in more than double the N<sub>2</sub>O fluxes in the latter ecosystem.

Several studies in lotic ecosystems have linked high NO<sub>3</sub> concentrations to elevated N<sub>2</sub>O production from incomplete denitrification (Andrews et al. 2021; Beaulieu et al. 2008; Mwanake et al. 2019). However, very few studies have connected N<sub>2</sub>O fluxes with direct measures of denitrification (e.g., Beaulieu et al. 2011), with most of the above studies inferring N<sub>2</sub>O sourced from denitrification based on positive correlations with NO<sub>3</sub> concentrations. Such inferences may be misleading, as N<sub>2</sub>O production from nitrification may also have a similar positive relationship with NO<sub>3</sub>, the end product of nitrification. When looking at the drivers of the significant longitudinal heterogeneities in N<sub>2</sub>O fluxes along the Mittelland Canal, we did find direct evidence of the critical role of denitrification in its production. This evidence was based on the significant positive relationship between N<sub>2</sub>O and N<sub>2</sub> fluxes, as positive N<sub>2</sub> fluxes are solely linked to the denitrification process and hence can be used to quantify its rates (Chen et al. 2014; McCutchan et al. 2003; Ritz et al. 2018; Wang et al. 2018).

In contrast to the canal ecosystem, longitudinal N<sub>2</sub>O hotspots downstream of the Rhine River were linked to processes other than denitrification. High N<sub>2</sub> fixation rates by cyanobacteria, autotrophic and heterotrophic diazotrophs, which supply fresh and bioavailable N, have been previously reported in freshwater environments (Geisler et al. 2022; Riemann et al. 2022). Within rivers, several studies have linked measures of N<sub>2</sub> undersaturation to significant rates of N<sub>2</sub> fixation by diazotrophs (Wang et al. 2021; Wu et al. 2013). This study found substantial downstream increases in N<sub>2</sub> uptake of up to 1747.31 mg m<sup>-2</sup> d<sup>-1</sup>, which more than doubled instream N<sub>2</sub>O fluxes. Like N<sub>2</sub>O, NH<sub>4</sub>-N, chlorophyll-*a*, and TOC concentrations, GPP and NEP rates also increased downstream of the Rhine. These findings implied significant N<sub>2</sub> fixation, possibly providing the NH<sub>4</sub>-N required for N<sub>2</sub>O production via nitrification. Such significant N<sub>2</sub> fixation rates have been previously reported in similar highly urbanized rivers in Beijing, with an N<sub>2</sub> undersaturation of up to 88% (Wang et al. 2021). We also found significant positive relationships of N<sub>2</sub>O with TOC concentrations, GPP, and NEP rates and their antagonistic relationship with N<sub>2</sub> fluxes, further supporting this argument.

**Table 2** Summary results of bivariate linear regression models indicating the relationship of water-physicochemical properties, N<sub>2</sub> fluxes, GPP, ER, and NEP rates with GHG fluxes (transformed with the natural logarithm) in the Rhine River and Mittelland Canal mainstem (harbors not included)

Dependent and independent variables	Rhine			Canal		
	<i>p</i> -value	Slope	<i>r</i> <sup>2</sup>	<i>p</i> -value	Slope	<i>r</i> <sup>2</sup>
<b>Ln CO<sub>2</sub> flux (mg m<sup>-2</sup> d<sup>-1</sup>)</b>						
ER (g O <sub>2</sub> m <sup>-2</sup> d <sup>-1</sup> )	0.02	-0.36	0.88			
<b>Ln CH<sub>4</sub> flux (mg m<sup>-2</sup> d<sup>-1</sup>)</b>						
NO <sub>3</sub> -N (mg L <sup>-1</sup> )	0.08	-0.26	0.30			
N <sub>2</sub> flux (mg m <sup>-2</sup> d <sup>-1</sup> )				0.10	2.38	0.80
<b>Ln N<sub>2</sub>O flux (mg m<sup>-2</sup> d<sup>-1</sup>)</b>						
DOC (mg L <sup>-1</sup> )	0.02	-0.89	0.52			
TOC (mg L <sup>-1</sup> )	0.04	0.05	0.38			
TSS (mg L <sup>-1</sup> )	0.05	0.01	0.36			
NH <sub>4</sub> -N (mg L <sup>-1</sup> )	0.06	4.96	0.30			
GPP (g O <sub>2</sub> m <sup>-2</sup> d <sup>-1</sup> )	0.02	0.40	0.88			
NEP (g O <sub>2</sub> m <sup>-2</sup> d <sup>-1</sup> )	0.01	0.51	0.93			
N <sub>2</sub> flux (mg m <sup>-2</sup> d <sup>-1</sup> )	0.02	-0.37	0.47	0.05	1.83	0.90

Only significant relationships (*p*-value < 0.05) and those with either positive or negative trends (*p*-values 0.05–0.10) with the GHG fluxes are shown. The complete table with all predictor variables and the *p*-values of the relationships is included in the supplementary materials (Table S3)

Cumulatively, these findings stress the need to include N<sub>2</sub> flux estimates in quantifying GHG from lotic ecosystems, as it has the potential to determine whether nitrogen is fixed through N<sub>2</sub> fixation or lost through denitrification, with severe consequences to both N and C cycling that results in the production of GHG from these ecosystems.

## Conclusion

Our study indicated that local hotspots of biogeochemical C and N cycling, point pollution sources, and harbors controlled the longitudinal GHG heterogeneities in two lotic ecosystems, albeit with different levels of importance depending on ecosystem type. These findings were primarily informed by combining GHG and N<sub>2</sub> concentration measurements and flux estimates with onsite water quality estimates from sensors, suggesting that such a methodology is most suitable for quantifying the drivers of large-scale GHG flux heterogeneities. However, our study was conducted only during the summer season, and as such, seasonal differences in discharge, temperature, and GHGs were not considered, which may additionally alter longitudinal GHG trends along the two lotic ecosystems as has been found in previous studies (Aho et al. 2022; Herreid et al. 2021; Mwanake et al. 2022, 2023a). For example, on the one hand, heavy precipitation-driven discharge events may tend to reduce local GHG hotspots due to shorter water residence times that inhibit internal GHG production processes but may increase the overall fluxes due to elevated gas transfer velocities and external GHG inputs, particularly in agricultural-dominated catchments (e.g., Mwanake et al. 2022, 2023b). On the other hand,

cold seasons may promote local GHG hotspots as microbial communities may face less competition for nutrients and organic carbon from plants (e.g., Herreid et al. 2021; Mwanake et al. 2023a).

**Supplementary Information** The online version contains supplementary material available at <https://doi.org/10.1007/s11356-024-33394-8>.

**Acknowledgements** We want to acknowledge the German Ocean Foundation for hosting our experiments during the Rhine Expedition 2023. Additionally, we thank the skipper Frank Schweikert and the staff of the Science & Media Vessel ALDEBARAN (Sofie Möhrle and Julia Kuhnle) for their tremendous support during the sampling campaign. The same thanks go to Dr. Madlene Stange, Dr. Leighton Thomas, and Michel Posanski from the Leibniz Institute, who were part of the Expedition. Furthermore, we thank the staff of the Flussgemeinschaft Rhein for establishing contact with the Landesamt für Natur, Umwelt und Verbraucherschutz NRW, and the Landesamt für Umwelt Rheinland-Pfalz, as well as the team of both agencies for providing continuous hourly data of oxygen concentrations and water temperature from the four water quality monitoring stations along the Rhine River.

**Author contribution** All authors contributed to the conceptualization and design of the work. Funding acquisition was done by Ralf Kiese. Ricky. M. Mwanake and Hannes K. Imhof prepared the field materials and collected the field data. Ricky. M. Mwanake conducted the formal analysis and wrote the first draft of the manuscript. All authors contributed to revising and editing the final manuscript draft.

**Funding** Open Access funding enabled and organized by Projekt DEAL. Infrastructure for the research was provided by the TERENO Bavarian Alps/Pre-Alps Observatory, funded by the Helmholtz Association through the joint program Changing Earth – Sustaining our Future (PoF IV) program of Karlsruhe Institute of Technology (KIT). Hannes K. Imhof was funded by the German Federal Ministry of Education and Research (BMBF) within the project Integrated Greenhouse Gas Monitoring for Germany (ITMS) – Module Sources & Sinks (Grant Number: 01LK2105D).

**Data availability** All data and data analyses codes of this manuscript will be made available upon request to the corresponding author.

## Declarations

**Ethical approval** Not applicable.

**Consent to participate** Not applicable.

**Consent for publication** Not applicable.

**Competing interests** The authors declare no competing interests.

**Open Access** This article is licensed under a Creative Commons Attribution 4.0 International License, which permits use, sharing, adaptation, distribution and reproduction in any medium or format, as long as you give appropriate credit to the original author(s) and the source, provide a link to the Creative Commons licence, and indicate if changes were made. The images or other third party material in this article are included in the article's Creative Commons licence, unless indicated otherwise in a credit line to the material. If material is not included in the article's Creative Commons licence and your intended use is not permitted by statutory regulation or exceeds the permitted use, you will need to obtain permission directly from the copyright holder. To view a copy of this licence, visit <http://creativecommons.org/licenses/by/4.0/>.

## References

- Aho KS, Raymond PA (2019) Differential response of greenhouse gas evasion to storms in forested and wetland streams. *J Geophys Res Biogeosci* 124(3):649–662. <https://doi.org/10.1029/2018JG004750>
- Aho KS, Fair JH, Hosen JD, Kyzivat ED, Logozzo LA, Weber LC, Yoon B, Zarnetske JP, Raymond PA (2022) An intense precipitation event causes a temperate forested drainage network to shift from N<sub>2</sub>O source to sink. *Limnol Oceanogr* 67(S1):S242–S257. <https://doi.org/10.1002/lno.12006>
- An S, Gardner WS, Kana T (2001) Simultaneous measurement of denitrification and nitrogen fixation using isotope pairing with membrane inlet mass spectrometry analysis. *Appl Environ Microbiol* 67(3):1171–1178. <https://doi.org/10.1128/AEM.67.3.1171-1178.2001>
- Andrews LF, Wadnerkar PD, White SA, Chen X, Correa RE, Jeffrey LC, Santos IR (2021) Hydrological, geochemical and land use drivers of greenhouse gas dynamics in eleven sub-tropical streams. *Aquat Sci* 83(2). <https://doi.org/10.1007/s00027-021-00791-x>
- Appling AP, Hall RO, Yackulic CB, Arroita M (2018) Overcoming equifinality: leveraging long time series for stream metabolism estimation. *J Geophys Res Biogeosci* 123(2):624–645. <https://doi.org/10.1002/2017JG004140>
- Battin TJ, Lauerwald R, Bernhardt ES, Bertuzzo E, Gener LG, Hall RO, Hotchkiss ER, Maavara T, Pavelsky TM, Ran L, Raymond P, Rosentreter JA, Regnier P (2023) River ecosystem metabolism and carbon biogeochemistry in a changing world. *Nature* 613(7944):449–459. <https://doi.org/10.1038/s41586-022-05500-8>
- Baulch HM, Dillon PJ, Maranger R, Schiff SL (2011) Diffusive and ebullitive transport of methane and nitrous oxide from streams: are bubble-mediated fluxes important?. *J Geophys Res: Biogeosci* 116(4). <https://doi.org/10.1029/2011JG001656>
- Beaulieu JJ, Arango CP, Hamilton SK, Tank JL (2008) The production and emission of nitrous oxide from headwater streams in the Midwestern United States. *Glob Chang Biol* 14(4):878–894. <https://doi.org/10.1111/j.1365-2486.2007.01485.x>
- Beaulieu JJ, Tank JL, Hamilton SK, Wollheim WM, Hall RO, Mulholland PJ, Peterson BJ, Ashkenas LR, Cooper LW, Dahm CN, Dodds WK, Grimm NB, Johnson SL, McDowell WH, Poole GC, Maurice Valett H, Arango CP, Bernot MJ, Burgin AJ, ... Thomas SM (2011) Nitrous oxide emission from denitrification in stream and river networks. *Proc Natl Acad Sci USA* 108(1):214–219. <https://doi.org/10.1073/pnas.1011464108>
- Begum MS, Bogard MJ, Butman DE, Chea E, Kumar S, Lu X, Nayna OK, Ran L, Richey JE, Tareq SM, Xuan DT, Yu R, Park JH (2021) Localized pollution impacts on greenhouse gas dynamics in three anthropogenically modified Asian river systems. *J Geophys Res: Biogeosci* 126(5). <https://doi.org/10.1029/2020JG006124>
- Bieroza M, Acharya S, Benisch J, ter Borg RN, Hallberg L, Negri C, Pruitt A, Pucher M, Saavedra F, Staniszevska K, van't Veen SGM, Vincent A, Winter C, Basu NB, Jarvie HP, Kirchner JW (2023) Advances in catchment science, hydrochemistry, and aquatic ecology enabled by high-frequency water quality measurements. *Environ Sci Technol* 57(12):4701–4719. <https://doi.org/10.1021/acs.est.2c07798>. (American Chemical Society)
- Bodmer P, Heinz M, Pusch M, Singer G, Premke K (2016) Carbon dynamics and their link to dissolved organic matter quality across contrasting stream ecosystems. *Sci Total Environ* 553:574–586. <https://doi.org/10.1016/j.scitotenv.2016.02.095>
- Borges AV, Darchambeau F, Lambert T, Bouillon S, Morana C, Brouyère S, Hakoun V, Jurado A, Tseng HC, Descy JP, Roland FAE (2018) Effects of agricultural land use on fluvial carbon dioxide, methane and nitrous oxide concentrations in a large European river, the Meuse (Belgium). *Sci Total Environ* 610–611:342–355. <https://doi.org/10.1016/j.scitotenv.2017.08.047>
- Brown AM, Bass AM, Skiba U, MacDonald JM, Pickard AE (2023) Urban landscapes and legacy industry provide hotspots for riverine greenhouse gases: a source-to-sea study of the River Clyde. *Water Res* 236:119969. <https://doi.org/10.1016/j.watres.2023.119969>
- Bussmann I, Koedel U, Schütze C, Kamjunke N, Koschorreck M (2022) Spatial variability and hotspots of methane concentrations in a large temperate river. *Front Environ Sci* 10. <https://doi.org/10.3389/fenvs.2022.833936>
- Chen N, Wu J, Chen Z, Lu T, Wang L (2014) Spatial-temporal variation of dissolved N<sub>2</sub> and denitrification in an agricultural river network, southeast China. *Agr Ecosyst Environ* 189:1–10. <https://doi.org/10.1016/j.agee.2014.03.004>
- Cornes RC, van der Schrier G, van den Besselaar EJ, Jones PD (2018) An ensemble version of the E-OBS temperature and precipitation data sets. *J Geophys Res: Atmos* 123(17):9391–9409. <https://doi.org/10.1029/2017JD028200>
- Deemer BR, Harrison JA, Li S, Beaulieu JJ, DelSontro T, Barros N, Bezerra-Neto JF, Powers SM, dos Santos MA, Vonk JA (2016) Greenhouse gas emissions from reservoir water surfaces: a new global synthesis. *Bioscience* 66(11):949–964. <https://doi.org/10.1093/biosci/biw117>
- Geisler E, Rahav E, Bar-Zeev E (2022) Contribution of heterotrophic diazotrophs to N<sub>2</sub> fixation in a eutrophic river: free-living vs. aggregate-associated. *Front Microbiol* 13. <https://doi.org/10.3389/fmicb.2022.779820>
- Gómez-Gener L, Rocher-Ros G, Battin T, Cohen MJ, Dalmagro HJ, Dinsmore KJ, Drake TW, Duvert C, Enrich-Prast A, Horgby Å, Johnson MS, Kirk L, Machado-Silva F, Marzolf NS, McDowell MJ, McDowell WH, Miettinen H, Ojala AK, Peter H, ... Sponseller RA (2021) Global carbon dioxide efflux from rivers enhanced by high nocturnal emissions. *Nat Geosci* 14(5):289–294. <https://doi.org/10.1038/s41561-021-00722-3>
- Herreid AM, Wymore AS, Varner RK, Potter JD, McDowell WH (2021) Divergent controls on stream greenhouse gas concentrations across a land-use gradient. *Ecosystems* 24(6):1299–1316. <https://doi.org/10.1007/s10021-020-00584-7>

- Ho L, Jerves-Cobo R, Barthel M, Six J, Bode S, Boeckx P, Goethals P (2022) Greenhouse gas dynamics in an urbanized river system: influence of water quality and land use. *Environ Sci Pollut Res* 29(25):37277–37290. <https://doi.org/10.1007/s11356-021-18081-2>
- Hotchkiss ER, Hall RO Jr, Sponseller RA, Butman D, Klaminder J, Laudon H, Rosvall M, Karlsson JJNG (2015) Sources of and processes controlling CO<sub>2</sub> emissions change with the size of streams and rivers. *Nat Geosci* 8(9):696–699. <https://doi.org/10.1038/ngeo2507>
- Hu M, Chen D, Dahlgren RA (2016) Modeling nitrous oxide emission from rivers: a global assessment. *Glob Chang Biol* 22(11):3566–3582. <https://doi.org/10.1111/gcb.13351>
- Jones MW, Peters GP, Gasser T, Andrew RM, Schwingshackl C, Gütschow J, Houghton RA, Friedlingstein P, Pongratz J, Le Quéré C (2023) National contributions to climate change due to historical emissions of carbon dioxide, methane, and nitrous oxide since 1850. *Sci Data* 10(1). <https://doi.org/10.1038/s41597-023-02041-1>
- Kana TM, Darkangelo C, Hunt MD, Oldham JB, Bennett GE, Cornwell JC (1994) Membrane inlet mass spectrometer for rapid high-precision determination of N<sub>2</sub>, O<sub>2</sub>, and Ar in environmental water samples. *Anal Chem* 66(23):4166–4170. <https://doi.org/10.1021/ac00095a009>
- Landesumweltamt Nordrhein-Westfalen (2002) Gewässergütebericht 2001, Berichtszeitraum 1995–2000. [https://www.lanuv.nrw.de/fileadmin/lanuv/publ/0\\_lua/gewgue01.pdf](https://www.lanuv.nrw.de/fileadmin/lanuv/publ/0_lua/gewgue01.pdf)
- Lauerwald R, Laruelle GG, Hartmann J, Ciais P, Regnier PAG (2015) Spatial patterns in CO<sub>2</sub> evasion from the global river network. *Glob Biogeochem Cycles* 29(5):534–554. <https://doi.org/10.1002/2014GB004941>
- Lauerwald R, Allen GH, Deemer BR, Liu S, Maavara T, Raymond P, Alcott L, Bastviken D, Hastie A, Holgerson MA, Johnson MS, Lehner B, Lin P, Marzadri A, Ran L, Tian H, Yang X, Yao Y, Regnier P (2023) Inland water greenhouse gas budgets for REC-CAP2: 1. State-of-the-art of global scale assessments. In *Global Biogeochemical Cycles* (Vol. 37, Issue 5). John Wiley and Sons Inc. <https://doi.org/10.1029/2022GB007657>
- Leng P, Li Z, Zhang Q, Koschorreck M, Li F, Qiao Y, Xia J (2023) Deciphering large-scale spatial pattern and modulators of dissolved greenhouse gases (CO<sub>2</sub>, CH<sub>4</sub>, and N<sub>2</sub>O) along the Yangtze River, China. *J Hydrol* 623:129710. <https://doi.org/10.1016/j.jhydrol.2023.129710>
- Li M, Peng C, Zhang K, Xu L, Wang J, Yang Y, Li P, Liu Z, He N (2021) Headwater stream ecosystem: an important source of greenhouse gases to the atmosphere. *Water Res* 190. <https://doi.org/10.1016/j.watres.2020.116738>
- Liu S, Kuhn C, Amatulli G, Aho K, Butman DE, Allen GH, Lin P, Pan M, Yamazaki D, Brinkerhoff C, Gleason C, Xia X, Raymond PA (2022) The importance of hydrology in routing terrestrial carbon to the atmosphere via global streams and rivers. <https://doi.org/10.1073/pnas.2106322119/-DCSupplemental>
- Marescaux A, Thieu V, Garnier J (2018) Carbon dioxide, methane and nitrous oxide emissions from the human-impacted Seine watershed in France. *Sci Total Environ* 643:247–259. <https://doi.org/10.1016/j.scitotenv.2018.06.151>
- McCutchan JH, Saunders JF, Pribyl AL, Lewis WM (2003) Open-channel estimation of denitrification. *Limnol Oceanogr Methods* 1(1):74–81. <https://doi.org/10.4319/lom.2003.1.74>
- Mulholland PJ, Fellows CS, Tank JL, Grimm NB, Webster JR, Hamilton SK, Martí E, Ashkenas L, Bowden WB, Dodds WK, McDowell WH, Paul MJ, Peterson BJ (2001) Inter-biome comparison of factors controlling stream metabolism. *Freshw Biol* 46(11):1503–1517. <https://doi.org/10.1046/j.1365-2427.2001.00773.x>
- Mwanake RM, Gettel GM, Aho KS, Namwaya DW, Masese FO, Butterbach-Bahl K, Raymond PA (2019) Land use, not stream order, controls N<sub>2</sub>O concentration and flux in the Upper Mara River Basin, Kenya. *J Geophys Res: Biogeosci* 124(11):3491–3506. <https://doi.org/10.1029/2019JG005063>
- Mwanake RM, Gettel GM, Ishimwe C, Wangari EG, Butterbach-Bahl K, Kiese R (2022) Basin-scale estimates of greenhouse gas emissions from the Mara River, Kenya: importance of discharge, stream size, and land use/land cover. *Limnol Oceanogr* 67(8):1776–1793. <https://doi.org/10.1002/lno.12166>
- Mwanake RM, Gettel GM, Wangari EG, Glaser C, Houska T, Breuer L, Butterbach-Bahl K, Kiese R (2023a) Anthropogenic activities significantly increase annual greenhouse gas (GHG) fluxes from temperate headwater streams in Germany. *Biogeosciences* 20(16):3395–3422. <https://doi.org/10.5194/bg-20-3395-2023>
- Mwanake RM, Gettel GM, Wangari EG, Butterbach-Bahl K, Kiese R (2023b) Interactive effects of catchment mean water residence time and agricultural area on water physico-chemical variables and GHG saturations in headwater streams. *Front Water* 5. <https://doi.org/10.3389/frwa.2023.1220544>
- Park JH, Nayna OK, Begum MS, Chea E, Hartmann J, Keil RG, Kumar S, Lu X, Ran L, Richey JE, Sarma VVSS, Tareq SM, Thi Xuan D, Yu R (2018) Reviews and syntheses: anthropogenic perturbations to carbon fluxes in Asian river systems — concepts, emerging trends, and research challenges. *Biogeosciences* 15(9):3049–3069. <https://doi.org/10.5194/bg-15-3049-2018>
- Park J-H, Lee H, Zhumabieke M, Kim S-H, Shin K-H, Kim B-K (2023) Basin-specific pollution and impoundment effects on greenhouse gas distributions in three rivers and estuaries. *Water Res* 236:119982. <https://doi.org/10.1016/j.watres.2023.119982>
- Peacock M, Audet J, Bastviken D, Futter MN, Gauci V, Grinham A, Harrison JA, Kent MS, Kosten S, Lovelock CE, Veraart AJ, Evans CD (2021) Global importance of methane emissions from drainage ditches and canals. *Environ Res Lett* 16(4). <https://doi.org/10.1088/1748-9326/abeb36>
- Piatka DR, Wild R, Hartmann J, Kaule R, Kaule L, Gilfedder B, Peiffer S, Geist J, Beierkuhnlein C, Barth JAC (2021) Transfer and transformations of oxygen in rivers as catchment reflectors of continental landscapes: a review. In *Earth-Science Reviews* (Vol. 220). Elsevier B.V. <https://doi.org/10.1016/j.earscirev.2021.103729>
- Raymond PA, Cole JJ (2001) Technical notes and comments gas exchange in rivers and estuaries: choosing a gas transfer velocity. In: *Estuarine research federation estuaries*, vol 24(2). [www.noaa.gov](http://www.noaa.gov)
- Raymond PA, Zappa CJ, Butman D, Bott TL, Potter J, Mulholland P, Laursen AE, McDowell WH, Newbold D (2012) Scaling the gas transfer velocity and hydraulic geometry in streams and small rivers. *Limnology and Oceanography: Fluids and Environments* 2(1):41–53. <https://doi.org/10.1215/21573689-1597669>
- Raymond PA, Hartmann J, Lauerwald R, Sobek S, McDonald C, Hoover M, Butman D, Striegl R, Mayorga E, Humborg C, Kortelainen P, Dürr H, Meybeck M, Ciais P, Guth P (2013) Global carbon dioxide emissions from inland waters. *Nature* 503(7476):355–359. <https://doi.org/10.1038/nature12760>
- Reay DS, Smith KA, Edwards AC (2003) Nitrous oxide emission from agricultural drainage waters. *Glob Chang Biol* 9(2):195–203. <https://doi.org/10.1046/j.1365-2486.2003.00584.x>
- Riemann L, Rahav E, Passow U, Grossart H-P, de Beer D, Klawonn I, Eichner M, Benavides M, Bar-Zeev E (2022) Planktonic aggregates as hotspots for heterotrophic diazotrophy: the plot thickens. *Front Microbiol* 13. <https://doi.org/10.3389/fmicb.2022.875050>
- Ritz S, Dähnke K, Fischer H (2018) Open-channel measurement of denitrification in a large lowland river. *Aquat Sci* 80(1). <https://doi.org/10.1007/s00027-017-0560-1>
- Rocher-Ros G, Stanley EH, Loken LC, Casson NJ, Raymond PA, Liu S, Amatulli G, Sponseller RA (2023) Global methane emissions from rivers and streams. *Nature*. <https://doi.org/10.1038/s41586-023-06344-6>

- Schade JD, Bailio J, McDowell WH (2016) Greenhouse gas flux from headwater streams in New Hampshire, USA: patterns and drivers. *Limnol Oceanogr* 61:S165–S174. <https://doi.org/10.1002/lno.10337>
- Silverthorn T, López-Rojo N, Foulquier A, Chanudet V, Detry T (2023) Greenhouse gas dynamics in river networks fragmented by drying and damming. *Freshw Biol* 68(12):2027–2041. <https://doi.org/10.1111/fwb.14172>
- Stelzer RS, Heffernan J, Likens GE (2003) The influence of dissolved nutrients and particulate organic matter quality on microbial respiration and biomass in a forest stream. *Freshw Biol* 48(11):1925–1937. <https://doi.org/10.1046/j.1365-2427.2003.01141.x>
- Teodoru CR, Nyoni FC, Borges AV, Darchambeau F, Nyambe I, Bouillon S (2015) Dynamics of greenhouse gases (CO<sub>2</sub>, CH<sub>4</sub>, N<sub>2</sub>O) along the Zambezi River and major tributaries, and their importance in the riverine carbon budget. *Biogeosciences* 12(8):2431–2453. <https://doi.org/10.5194/bg-12-2431-2015>
- Wang G, Wang J, Xia X, Zhang L, Zhang S, McDowell WH, Hou L (2018) Nitrogen removal rates in a frigid high-altitude river estimated by measuring dissolved N<sub>2</sub> and N<sub>2</sub>O. *Sci Total Environ* 645:318–328. <https://doi.org/10.1016/j.scitotenv.2018.07.090>
- Wang G, Xia X, Liu S, Wang J, Zhang S (2021) Low diffusive nitrogen loss of urban inland waters with high nitrogen loading. *Sci Total Environ* 789. <https://doi.org/10.1016/j.scitotenv.2021.148023>
- Wu J, Chen N, Hong H, Lu T, Wang L, Chen Z (2013) Direct measurement of dissolved N<sub>2</sub> and denitrification along a subtropical river-estuary gradient, China. *Mar Pollut Bull* 66(1):125–134. <https://doi.org/10.1016/j.marpolbul.2012.10.020>
- Yao Y, Tian H, Shi H, Pan S, Xu R, Pan N, Canadell JG (2020) Increased global nitrous oxide emissions from streams and rivers in the Anthropocene. *Nat Clim Chang* 10(2):138–142. <https://doi.org/10.1038/s41558-019-0665-8>. (**Nature Research**)
- Zhang M, Chadwick MA (2022) Influences of elevated nutrients and water temperature from wastewater effluent on river ecosystem metabolism. *Environ Processes* 9(3). <https://doi.org/10.1007/s40710-022-00597-5>

**Publisher's Note** Springer Nature remains neutral with regard to jurisdictional claims in published maps and institutional affiliations.